Am J Cancer Res 2023;13(1):25-44
www.ajcr.us /ISSN:2156-6976/ajcr0145609

Original Article

Improved platform for breast cancer circulating tumor cell enrichment and characterization with next-generation sequencing technology

Catalin Mihalcioiu[1], Jiarong Li[1], Dunarel Badescu[3], Anne Camirand[1], Nathaniel Kremer[1], Nicholas Bertos[1], Atilla Omeroglu[1], Michael Sebag[1], John Di Battista[1], Morag Park[2], Jiannis Ragoussis[3], Richard Kremer[1]

[1]Department of Medicine, McGill University Health Centre, Glen Site, 1001 Boul. Décarie, Mail Drop EM1.3229, Montréal, Québec, H4A 3J1, Canada; [2]Breast Cancer Functional Genomics Group, Rosalind and Morris Goodman Cancer Centre, McGill University, Montréal, Québec, Canada; [3]McGill University Génome Centre, Department of Human Genetics, Montréal, Québec, Canada

Received July 28, 2022; Accepted September 29, 2022; Epub January 15, 2023; Published January 30, 2023

Abstract: Circulating tumor cells (CTCs) represent cells shed from the primary tumor or metastatic sites and can be used to monitor treatment response and tumor recurrence. However, CTCs circulate in extremely low numbers making in-depth analysis beyond simple enumeration challenging when collected from peripheral blood. Furthermore, tumor heterogeneity, a hallmark of many tumors, especially breast cancer, further complicates CTC characterization. To overcome this limitation, we developed a platform based on the large-scale isolation of CTCs by apheresis, allowing us to collect CTCs in large numbers, which were preserved live in liquid nitrogen for further characterization. Flow cytometry followed by cell sorting (FACS) was performed using a combination of antibodies directed against cell surface markers of white blood cells (CD45) and epithelial tumor cells (CK8). Analysis of subpopulations CD45+/- and CK8+/- by bulk RNA sequencing (RNAseq) and the CD45-/CK8 positive population by single-cell RNAseq was performed. The CD45- population was enriched using CD45 magnetic beads separation and examined by IHC for pan-cytokeratin and immunofluorescence (IF) for specific markers, including the elusive circulating cancer stem cells (CSCs). CSC-rich mammospheres were grown in vitro for further analysis and treated to examine their response to chemotherapeutic agents. Finally, mammospheres were transplanted into the mammary fat pad and bone of immunodeficient mice to examine tumor growth in vivo. This platform enables the detection and collection of CTCs in early and late-stage breast cancer patients of every subtype. Markers including CD44/24, ALDH1 and CXCR4 were identified by IF and showed high expression following mammosphere culture, which responded predictably to chemotherapeutic agents. Mammospheres were also transplanted into nude mice and induced tumors in the mammary fat pad and bone following intra-tibial transplantation. Finally, bulk RNA analysis of the FACS isolated CD45+/- and CK8+/- cells showed a clear separation of CD45- away from CD45+ populations. Single-cell RNAseq of the FACS isolated CD45-/CK8+ cells showed the presence of 4-5 clusters, confirming the high degree of heterogeneity of CTCs. Our platform for large-scale isolation of CTCs using apheresis is suitable for an in-depth analysis of the cancer phenotype and may eventually allow evaluation in real-time of the disease process to optimize cancer regimens.

Keywords: Circulating tumor cell, breast cancer, liquid biopsy, apheresis, single-cell RNA sequencing, epithelial-to-mesenchymal transition, xenografts

Introduction

In cancer patients with malignant tumors, morbidity and mortality often do not result from the primary tumor growth but rather from metastatic proliferation [1]. Metastases are initiated by cancer cells that are released from the primary tumor into the lymphatic system or the peripheral circulation and migrate to distal sites in the body [2]. Many types of solid cancers shed circulating tumor cells (CTCs) from their primary tumors or from their metastases, and these CTCs can be accessed from blood through minimally invasive intervention [3]. Early studies in breast, prostate and colorectal cancer cases have revealed that enumeration of CTCs allows prediction of metastasis and monitoring of therapeutic response [4-11].

However, beyond simple enumeration, a substantial amount of crucial supplementary information can be gathered by isolating CTCs and conducting genomic, transcriptomic, epigenetic, and proteomic analyses as well as *in vitro* and xenograft studies [2, 12]. Such efficient analysis of isolated CTCs allows longitudinal studies of patients and the information obtained is highly useful in the context of drug resistance acquisition and in the identification of new molecular targets [13, 14].

Because CTCs represent an easily obtainable "liquid biopsy" that can be collected repeatedly as needed and with much less patient discomfort than traditional tumor tissue biopsy, a vast research effort is underway to develop improved methods for CTC purification and analysis from blood. However, two main characteristics of CTCs hinder easy clinical analysis. First, CTCs are very rare: in a cohort of 350 patients with metastatic breast cancer, almost all patients had 5 or less CTCs per 7.5 ml of peripheral blood, and only 1.43% of patients had 500 or more [15]. Second, CTCs are heterogeneous, with several subpopulations that not only express diverse cell surface markers but whose marker expression varies over time while in circulation [16, 17]. Furthermore, CTCs can be released from primary tumors either as single cells or as rare clusters of two to fifty or more cells. CTC clusters present rapid clearance within distal organs and display higher metastatic potential compared to single CTCs, as confirmed in mouse models and by the adverse prognosis in patients with high numbers of such clusters [18].

Whether single or in clusters, CTCs issued from primary tumors have partially or completely undergone a cellular process called epithelial to mesenchymal transition (EMT) that allows cells to lose epithelial characteristics, gain mesenchymal properties and become motile and invasive. According to the EMT/MET model for metastasis, upon invasion of the distal target tissue, CTC cells reverse the EMT process by undergoing mesenchymal to epithelial transition (MET) then settle into the new microenvironment and form metastases [17, 19]. In contrast, according to the collective migration model, CTCs in various stages of EMT migrate in clusters with mesenchymal cells facilitating entry into distal sites, and epithelial cells generating the metastases [20]. The EMT/MET model and collective migration model are not mutually exclusive and tumor cells may switch between the two mechanisms under certain circumstances, or the two mechanisms may act synergistically to effect metastases [20].

In a meta-analysis of 50 studies (comprising 6712 breast cancer patients), the enumeration of CTCs pre- and post-treatment in patient blood has been shown to be a reliable indicator for monitoring disease progression probability as well as survival period [21]. Although CTC numbers can serve as an indicator to monitor the effectiveness of treatments and guide subsequent therapies in breast cancer, a simple overall count of the general CTCs population does not cover all possible therapeutic insights. Consequently, efforts now focus on detection and characterization of the crucial CTC subpopulation responsible for successful metastasis, and a suitable solution is required to isolate CTCs in sufficient numbers for in-depth characterization.

Current methods for CTC purification are mostly based on positive/negative immunoselection or on biophysical properties such as size, charge, density or deformability [2]. The most common technique for epithelium-derived cancers uses positive immunoselection of epithelial cell adhesion marker molecule (EpCAM) [22]. A significant shortcoming to this method, particularly in breast cancer, rises from the fact that EpCAM level not only varies significantly between cancer subtypes but that its expression is associated with an unfavorable prognosis in some subtypes and a favourable one in others making it context-dependent [23]. Furthermore, the EMT process likely removes the EpCAM marker from the CTC population and causes the cells to express mesenchymal markers instead [24]. Consequently, EpCAM-based detection may under-estimate CTC numbers and miss critical subpopulations. Other differentiation markers such as the prostate-specific antigen (PSA), human epidermal growth factor receptor 2 (HER2) and epidermal growth factor receptor (EGFR) that are also used for positive selection may not detect undifferentiated CSCs [17]. Size-based filtration methods, on the other hand, are based on the large size of differentiated CTCs, and only yield the largest and more differentiated CTCs but do not capture the entire CTC population which are heterogeneous in size. The technical limitations of current purification methods suggest a need for more comprehensive isolation techniques

such as negative immunoselection for the hematopoietic marker CD45 which is not associated with cancer cells, but allows removal of leukocytes and does not exclude any CTC subpopulations [25]. Cytokeratins (CKs) are cytoskeleton proteins expressed on epithelial tissue including metastatic tumor cells, epithelial CTCs and mesenchymal CTCs with residual CK expression, and are frequently used in CTC detection [16, 26].

Apheresis is a centrifugation-based procedure during which blood from a patient is passed through a medical device that separates one or more components and returns the balance of the blood to the circulation [27]. This method allows enrichment of a peripheral blood mononuclear cells (PBMCs) fraction that contains CTCs shed in the blood by the patient's tumor [28]. Since a large proportion of the blood supply is processed during apheresis, the method greatly increases the number of CTCs collected from patients compared to that obtained from the standard 7.5 ml blood sample commonly used for CTC analysis [29, 30]. Apheresis has been used for enrichment of CTCs from peripheral blood in a number of cancer types, such as lung [31], prostate [32], colorectal [33], breast [34], gastric [35] and biliary [36] and non-metastatic breast cancer patients [37, 38].

In the present study, we describe the development of an apheresis-based purification platform that collects CTCs in large numbers from breast cancer patients and captures CTCs with tumor-forming ability. The apheresis step is followed by concentration of PBMC cells on Ficoll-Paque Plus gradients and by magnetic bead selection for CD45-negative and cytokeratin 8 (CK8)-positive markers. Here, we demonstrate our platform's utility in gathering concentrated cell subpopulations that can be further purified and characterized for crucial markers and used for *ex vivo* tests. We also demonstrate that these cell populations can be used for single-cell RNA analysis through next-generation sequencing, an analysis step that further subdivides CTC populations in distinct expression categories. We provide a proof-of-principle method that can be used to provide real-time, non-invasive, longitudinal monitoring for cancer patients and to screen the effects of pharmaceutical compounds *ex vivo*. We suggest that our apheresis-based collection platform can be used as a cost-effective approach to personalized medicine.

Materials and methods

Patient selection

Early and late-stage female breast cancer patients seen at the Breast Centre of the Royal Victoria Hospital were asked for informed consent for sample collection, investigation of previously archived specimens, and for follow-up. Patients with different receptor status, diagnosis, grade of the primary tumor, stage and metastasis sites were selected for screening. Full clinical, epidemiological and pathological information (tumor grade, ER, PR, Her2/neu status, histological subtype, and grade) for patients entered in this study was collected via chart review. All results are kept in a database in accordance with institutional policies on patient record confidentiality. Regular chart review was used to detect changes in patient status. Patients found to be CTC-positive by peripheral blood screening were approached and offered whole blood volume apheresis.

Preliminary screening of peripheral blood mononuclear cells (PBMCs) by CD45 negative selection and immunohistochemistry

Peripheral blood (15 ml) was drawn from consenting patients. The first 5 ml of blood sampled was discarded to avoid potential contamination with normal epithelial cells during venipuncture. The remaining 10 ml collected in 1 mM EDTA was used for CTC screening. The sample was diluted 1:1 with PBS (Wisent Bioproducts, St Bruno, QC) containing 2% FBS (Life Technologies, Burlington, ON), layered over an equal volume of Ficoll Paque PLUS (71-7167-00, GE Healthcare, Canada), and centrifuged at 400×g 30 minutes at 18-20°C. The mononuclear cells layer was collected and diluted with 2% FBS in PBS and re-centrifuged. The supernatant was discarded and the pellet consisting of PBMCs was resuspended in PBS. Cell count was performed with a Z1 Particle Coulter Counter® (Beckman Coulter Canada, Mississauga, ON) before CD45 negative cell enrichment. Negative selection enrichment for CD45- cells was conducted on 1×10^7 PBMCs resuspended in RoboSep buffer (1 mM EDTA, 2% FBS in PBS) using a RoboSep separator with magnetic beads coated with anti-human CD45 antibodies (Easy Sep Human CD45 depletion kit, Stem Cell Technologies, Vancouver, BC) according to manufacturers instructions. CD45- cells were resuspended in

PBS at 1×10^6/ml and centrifuged at 1000 rpm 5 minutes in Shandon cytofunnels (Thermo Fisher Scientific Inc., Waltham, MA, USA) using a Cytospin Cytocentrifuge (Fisher Scientific Canada) and deposited (0.1 ml per spot) onto super frost plus microscope slides (Fisher Scientific Canada, Whitby, ON). The slides were air-dried overnight, fixed with cold acetone 10 minutes, air-dried and either stored at -80°C or immunostained for pan-cytokeratin A45-B/B3 using the EpiMet epithelial cell detection kit (AS Diagnostic, Hückeswagen, Germany) which detects a common epitope of cytokeratins 8-18, 8-19 and CK7.

Blood apheresis

The procedure was carried out using a Cobe Spectra instrument (Terumo Blood and Cell Technologies, Lakewood, CO) in a clinical apheresis facility at the McGill University Health Centre, under the supervision of experienced nurses and an attending physician. Briefly, 5 liters of whole anticoagulated (1 mM EDTA) blood was continuously processed over a 3-hour session to centrifuge and separate blood components by specific gravity. Nucleated cells (white blood cells and CTCs) are collected while non-nucleated cells (red blood cells and platelets) are returned to the patient. While this technique involves the insertion of a large-bore peripheral venous catheter, it has been shown to pose minimal risk to patients. The procedure takes 3-4 hours to complete and is generally well-tolerated [39]. Blood tests were conducted before apheresis and within 1 month after the apheretic procedure. White blood cell (WBC) values were observed to have slightly fluctuated up or down after apheresis: we observed that 9% of patients had identical WBC values, 50% had slightly lower values (average -16% of pre-apheresis values) and 41% had higher WBC values (+19.9% of pre-apheresis values). It therefore appears that WBC counts return to normal levels after the procedure. No adverse events occurred in any of the patients subjected to apheresis. Approximately 200 ml of apheresis nucleated cells product was collected per selected patient.

PBMC purification and concentration

Anticoagulant-treated nucleated apheresis product fraction (200 ml) was diluted with an equal volume of PBS (Wisent Bioproducts, St Bruno, QC) containing 2% FBS (Life Technologies, Burlington, ON). The diluted sample was layered over half the volume of Ficoll Paque PLUS (GE HealthCare, Mississauga, ON) and centrifuged at 400×g 30 minutes at 18-20°C. The lymphocyte layer was collected, diluted with PBS containing 2% FBS and re-centrifuged at 400×g 10 minutes at 18-20°C. The supernatant was removed and the pellet containing nucleated cells resuspended in PBS to a final volume of 60 ml. Cell count was performed with a Z1 Particle Coulter Counter® (Beckman Coulter Canada, Mississauga, ON). A 30 ml sample of the PBMC was aliquoted in fractions containing CTCs (1×10^8 cells per ml), resuspended in freezing medium (90% serum, 10% DMSO) and stored in liquid nitrogen until further analysis by FACS or flow cytometry. The remaining 30 ml was subjected to RoboSep enrichment.

RoboSep CD45 exclusion

Following Ficoll concentration, the apheresis material was subjected to negative selection enrichment using a RoboSep separator as described above. Briefly, 1×10^9 PBMC cells were resuspended in RoboSep buffer (1 mM EDTA, 2% FBS in PBS) to a final concentration 1×10^8 per ml, and depleted using the Easy Step Human CD45 depletion kit (Stem Cell Technologies, Vancouver, BC) according to manufacturer's instructions. CD45- cells were counted and cell concentration calculated as above. 20×1 ml aliquots containing 5×10^6 cells/ml were cryo-preserved in freezing medium (90% serum, 10% DMSO). Aliquots were used for immunofluorescence and mammosphere culture studies. This negative selection process allows a 10-fold enrichment of tumor cells. Positive identification of CTCs as epithelial cells was performed by staining a dried aliquot with the Epimet Epithelial Cell Kit (Micromet, Munich, Germany) according to kit instructions, on Cytospin Immunoselect Adhesion Slides (Squarix, Marl, Germany). The Epimet kit uses the murine pan-cytokeratin A45-B/B3 monoclonal antibody directed against a common epitope of cytokeratin polypeptides.

Reproducibility assessment

The reproducibility of the method was determined on repeated measurements of CD45 negative fractions from various patients. The coefficient of variation was 3.8% (intra assay) and 15% (inter assay).

Immunofluorescence (IF), confocal microscopy and immunohistochemistry (IHC)

For immunofluorescence-confocal microscopy, cells grown in culture or isolated by Robosep were resuspended in PBS (1×10^6 cells per ml), and 0.1 ml aliquots deposited on Super Frost Plus microscope slides (ThermoFisher) using Shandon microfunnels (ThermoFisher). The slides were air-dried overnight, fixed with cold acetone for 10 minutes, air-dried 30 minutes and immediately subjected to immunostaining or stored at -80°C. For immunostaining, the SK-4100 kit (Vector Labs, Brockville ON) was used. Cells were reacted with diaminobenzidine and analysed with a Leica DMR microscope. For immunofluorescence, results were analysed with an LSM 510 Meta confocal microscope (Carl Zeiss, Jena, Germany). The antibodies used were: anti-human CK8/18 (Ab 17139, Abcam, Cambridge, UK) and ALDH1 (polyclonal PA 5-34901, InVitrogen, Waltham, MA).

Mammosphere culture

Aliquots of post RoboSep CD45- cells (approximately 5×10^6 cells expected to contain 50 to 3000 CTCs depending on the patient and assuming a 10-fold enrichment following Robosep negative selection) were plated in ultra low adherence 6-well culture dishes (Corning Life Sciences) with 3 ml of mammocult medium/well with proliferation supplement (4 µg/ml heparin, 0.48 µg/ml hydrocortisone, 1% penicillin/streptomycin, StemCell Technologies, Vancouver, BC), and incubated at 37°C in a 5% CO_2 incubator. Cells were fed with an additional 1 ml of mammocult medium after 1 week. After two weeks, mammospheres displayed size >40 µm and were collected by centrifugation (10 minutes at 1000 g). The supernatant was removed, 4 ml of trypsin was added to the pellet and the mammospheres incubated at 37°C 10 minutes with up and down pipetting at 0, 5, and 10 minutes. The trypsin was neutralized by addition of 16 ml DMEM containing 10% FBS and 1% penicillin/streptomycin, and the single cells were counted using a Coulter counter (Beckman Coulter Technologies). 30,000 cells were used to prepare slides and the remaining 30-50,000 cells were transferred to a new low-attachment plate for continued expansion with passages every second week to continue amplification to the third generation. Through this approach, a near 100-fold expansion of the initial cell population was achieved (i.e. 5,000 to 300,000 cells were obtained from the original 50 to 3000 CTCs).

For IF, mammospheres were fixed in paraformaldehyde 4% for 15-30 minutes at RT, washed with PBS and permeabilized with 0.3% Triton X-100 for 1 h. Slides were incubated with the primary antibodies O/N then washed and reacted with secondary Ab. Results were analysed with an LSM 780 Meta confocal microscope (Carl Zeiss Microimaging). The following antibodies were used for staining: from Abcam (Cambridge, UK): anti human CK8/18 (Ab17139). From eBiosciences (Montréal, QC): anti-CD44 human/mouse (Ab 17-0441-82). From InVitrogen (Waltham, MA): rabbit anti-human vimentin monoclonal antibody SP20 (CMA5-14564), EpCam CD326 monoclonal antibody 1B7 (14-9326-82), and anti-ALDH1 polyclonal Ab (PA5-34901). From R and D Systems (Minneapolis, MN): anti human CXCR4 (MAB 170). Secondary antibodies were all from InVitrogen: goat anti-Mouse IgG (H+L) Cross-Adsorbed Secondary Antibody, Alexa Fluor 568 (A-11004), donkey anti-Mouse IgG (H+L) Highly Cross-Adsorbed Secondary Antibody, Alexa Fluor 488 (A-21202), goat anti-Rabbit IgG (H+L) Cross-Adsorbed Secondary Antibody, Alexa Fluor 488 (A-11008), donkey anti-Rabbit IgG (H+L) highly Cross-Adsorbed Secondary Antibody, Alexa Fluor 546 (A10040), donkey anti-Mouse IgG (H+L) Highly Cross-Adsorbed Secondary Antibody, Alexa Fluor 647 (A-31571), goat anti-rabbit IgG (H+L) Highly Cross-Adsorbed Secondary Antibody, Alexa Fluor 405 (A-31556).

Drug treatment of mammospheres

Aliquots of post RoboSep CD45- cells (approximately 5×10^6 cells containing 1000-3000 CTCs) were plated in ultra low adherence 6-well culture dishes (Corning Life Sciences) with 3 ml of mammocult medium/well with proliferation supplement (4 µg/ml heparin, 0.48 µg/ml hydrocortisone, 1% penicillin/streptomycin, StemCell Technologies, Vancouver, BC), and incubated at 37°C in a 5% CO_2 incubator. Cells were fed with an additional 1 ml of mammocult medium after 1 week. After two weeks in culture, the size of the mammospheres was >40 µm in diameter and they were collected. After two further subcultures in mammocult medium

to eliminate residual white blood cells, mammospheres were collected by centrifugation and used for apoptosis drug testing.

For drugs tests, an equal volume of the test compounds was added to the mammospheres plates in mammocult medium and the plates incubated for a further 48 hours. The drugs used were: paclitaxel (Taxol®, Bristol-Myers Squibb, Montréal QC) at final concentration 10 nM, a drug which causes cell death due to chromosome missegregation on multipolar spindles [40]; trastuzumab (Herceptin®, Genentech, Inc., South San Francisco, CA) at final concentration 10 μg/ml, a monoclonal antibody against HER-2 positive cancers: or doxorubicin (Pfizer, Montréal QC) at final concentration 10 uM, an intercalating drug that interferes with DNA and RNA synthesis. Mammospheres were collected, trypsinized and analyzed by flow cytometry for apoptosis.

Flow cytometry analysis

Cells were stained according to standard protocols with annexin V (BD Biosciences, Mississauga, ON) and 7-amino-actinomycin D (7-AAD, Abcam 228563) viability dye which allows to distinguish between necrotic and apoptotic cells since intact cells in early apoptosis exclude 7-AAD while late apoptotic cells will stain with 7-AAD. Stained cells were analyzed using a LSRF Fortessa flow cytometer (BD Biosciences).

Xenografts

Post RoboSep selection CD45- cells were put in mammosphere culture as described above. Mammospheres were trypsinized and subcultured every second week to continue amplification to the third generation. After trypsinization and counting, 10,000 cells were injected either in the fourth mammary fat pad (MFP) or intratibially into 8-week old SCID immunodeficient mice (5 female mice per MFP group and 5 per intratibial group, Jackson Laboratories, Bar Harbor, ME) as described in [41]. Control mice were sham injected. The MFP-injected mice were sacrificed 8 weeks post-injection, mammary gland xenografts were collected and tissue slices immediately fixed in 10% neutral buffered formalin solution (Sigma) for 4 hours, embedded in paraffin and analyzed by standard hematoxylin and eosin (H&E) staining. Intra-tibially injected animals were sacrificed 8 weeks after injection and bones were fixed in 70% ethanol then scanned by computerized tomography (CT scan) at the Center for Bone and Periodontal Research, McGill University, with a SkyScan 1072 at 40x magnification. Fixed bones were also embedded in methylmethacrylate (J-T Baker, Phillipsburg, NJ), placed on gelatin-coated glass slides and stained with hematoxylin and eosin (H&E) stain using standard protocols.

FACS isolation based on CK8 positivity and CD45 exclusion

Post-apheresis PBMCs cells were selected for viability using the eFluor 506 viability dye (eBioscience, ThermoFisher) using a FACS-Aria II cell sorting instrument (BD Biosciences, Mississauga, ON). Viable cells were sorted for CD45 exclusion and CK8 positivity as follows: PMBCs were stained with 4',6-diaminido-2-phenylindole (DAPI) and anti-CD45-APC-Cy antibody (BD Biosciences). Gated living cells were stained with an anti-CK8-PercP-efluor 710 antibody (eBioscience). CD45+ subpopulations (CK8+ and -) were also collected for RNA analysis.

RNA sequencing (bulk)

200-cell or 1000-cell aliquots from patient 22 (TNBC) were lysed and cDNA synthesis initiated using the SMARTer amplification method (Clontech/TakaraBio, Mountain View, CA). Cells from the CD45+CK8-, CD45+CK8+, CD45-CK8- and CD45-CK8+ were analysed. The cDNA preparations were used to prepare libraries for next generation sequencing by Nextera's tagmentation method (Illumina, SanDiego CA). Libraries were sequenced with a HiSeq 2500 Ultra-high Output Sequencer (Illumina) at a rapid sequencing pipeline. 10^6 reads from the samples allowed for comprehensive bioinformatics analysis (Genome Sciences, McGill University and Genome Quebec Innovation Center, Montréal, Canada).

RNA sequencing (single cells)

A 5 μl suspension of 200-1000 CD45-CK8+ cells from patient 22 (TNBC) was stained with viability Live/Dead stain (Thermofisher), checked under a fluorescent microscope and counted with a Moxi Z cell counter (Thermofisher, CAN) that also estimates cell size. A 5-ml volume of sorted CD45-CK8+ cells was loaded on a 5-10 micrometer Fluidigm C1 single cell isola-

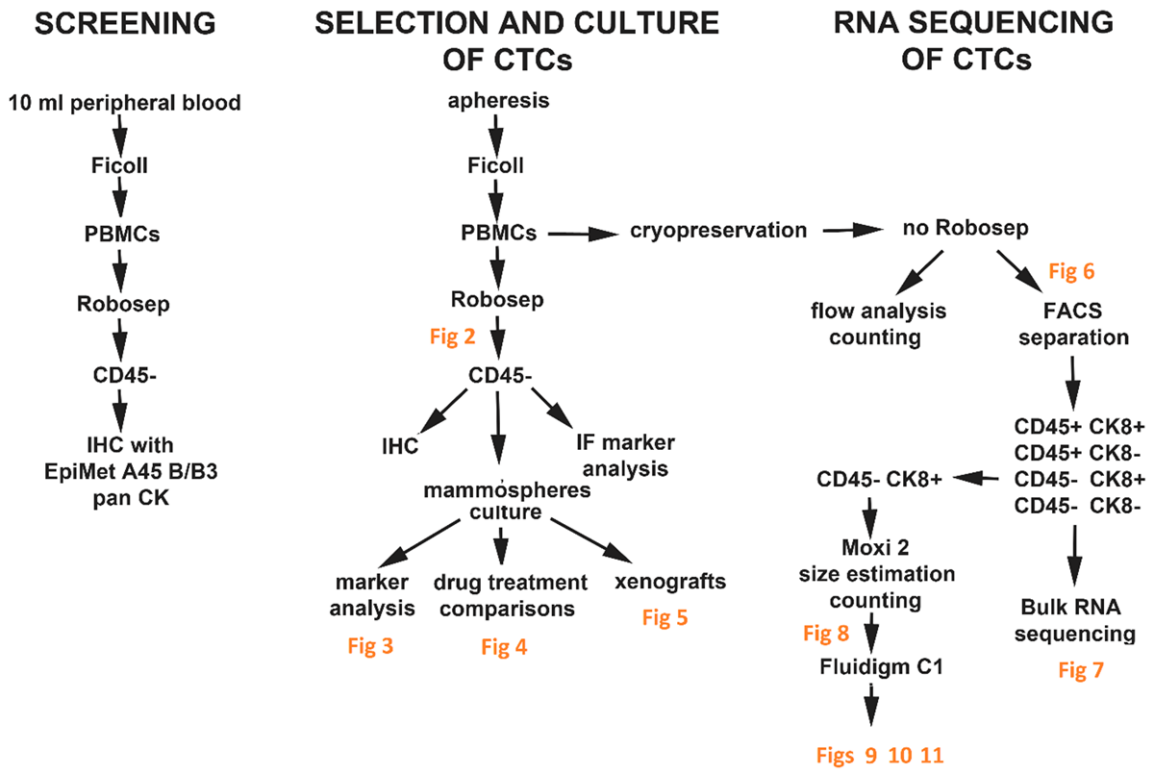

Figure 1. Platform description: Screening of patients (left) is used to identify candidates for full-scale apheresis analysis. (Center) Apheresis of selected patient blood is followed by Ficoll density gradient to obtain PBMCs. Robosep enrichment of CD45- cells is followed by marker analysis, in vitro culture and xenograft experiments. (Right) PBMCs can also be analysed by flow cytometry or partitioned according to CD45 and CK8 status and used in RNA sequencing.

tor (Fluidigm, San Francisco, CA). Between 60-96 cells were captured from each sample as single cells. To maintain full viability, cells were analysed within 5 minutes of capture using an automated scanning fluorescent imaging system (EVOS FL, ThermoFisher CAN) and single cells scored for cytokeratin expression. Viable cells appeared as green and CK8 positive cells were red. Double-positive cells appeared yellow. The cells were then lysed in the chip, and in-chip cDNA synthesis initiated using the SMARTer amplification method (Clontech/TakaraBio, Mountain View, CA) resulting in amplification of single-cell polyA+ from sub-picogram to nanogram levels of cDNA. The chip cDNA was used to prepare libraries for next generation sequencing by Nextera's tagmentation method (Illumina, SanDiego CA) which is suitable for nanogram amounts of DNA. Libraries were sequenced with a HiSeq 2500 Ultra-high Output Sequencer (Illumina) at a rapid sequencing pipeline as described above. A minimum of 1 million reads/single cell sample allowed for comprehensive bioinformatics analysis (Genome Sciences, McGill University and Genome Quebec Innovation Center, Montréal, Canada).

Statistical analysis

All statistical analyses for intra assay and inter assay variation were performed using Instat Software (GraphPad Software).

Study approval

The animal studies were approved by the McGill University Animal Compliance Office, institutional approval number 7713.

Results

Platform description

After initial patient screening (**Figure 1** left), two parallel protocols can be followed. The first protocol analyses post-apheresis CD45 negative leukocyte-free PBMCs from selected patients for presence of CTC markers and cap-

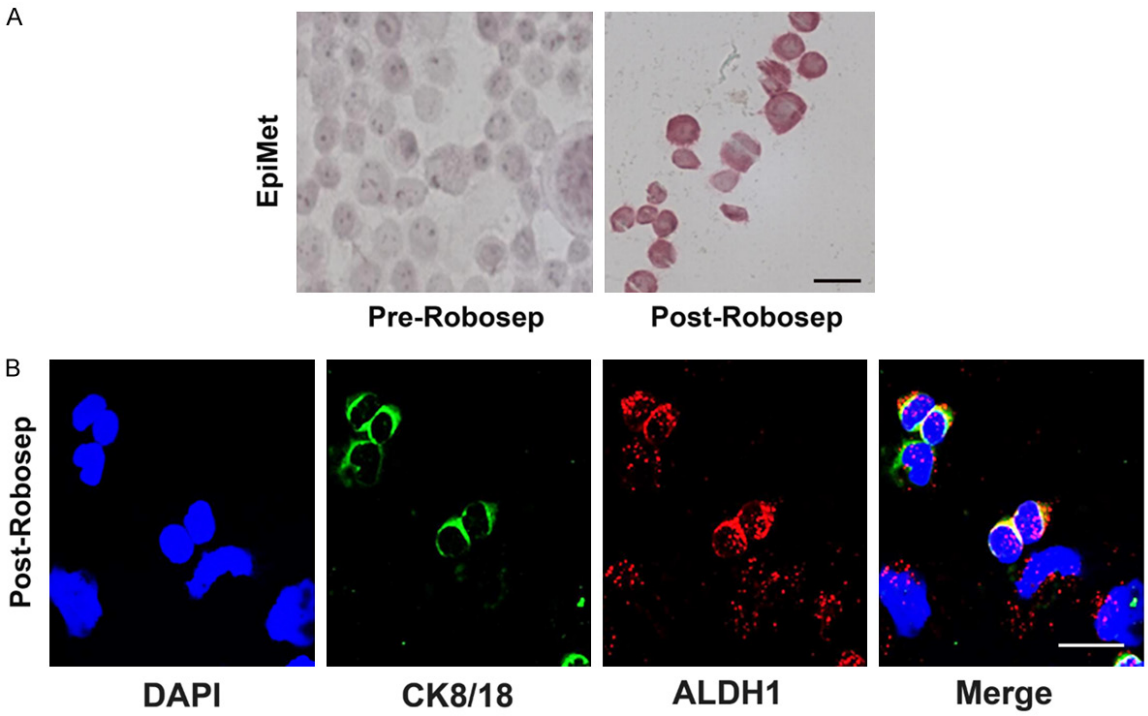

Figure 2. Analysis of post-apheresis, post-Ficoll PBMCs: (A) EpiMet cytokeratin staining of patient PBMCs before (left) and after (right) CD45 depletion by Robosep. (B) Post-Robosep cells are enriched in CK8/18 and ALDH1 markers. Scale bar 50 µm.

acity for mammosphere formation as well as xenograft transplantation (**Figure 1** center). In parallel, the second protocol divides through FACS separation the total PBMC population into CD45+ or - and CK8+ or - subgroups that are used for bulk or single-cell RNA sequencing (**Figure 1** right).

Selection and culture of CTCs

Peripheral blood taken from patients and filtered through apheresis was centrifuged over Ficoll and the PMBC fraction was depleted of CD45+ cells by Robosep (Stem Cells Technology). The result was an enrichment in cells positive for EpiMet stain (A45-B/B3 broad range pan-cytokeratin) indicating epithelial origin (**Figure 2A**). The Post-Robosep EpiMet-positive population was observed by IF to be enriched in cells staining positively for CK8/18 and ALDH1 (**Figure 2B**). The presence of cell clusters containing two or more cells was also commonly detected. We identified cells that display a double positive staining (CK8/ALDH1) as a likely CSC phenotype. These results reveal enrichment in cells that are CD45- CK8/18+ ALDH1+ and indicate a CSC-enriched population.

Mammosphere formation

A triple-negative patient (number 22, see **Table 1**) was selected to conduct more detailed analyses. When her CD45- cells were cultured *in vitro,* they consistently exhibited the capacity to proliferate either as adherent cells or, in absence of serum, as mammospheres (**Figure 3A-C**). Mammospheres became more abundant with each passage and immunofluorescence/confocal microscopy revealed a positive staining pattern for CK8, EpCAM, ALDH1, CD44, and CXCR4, indicative of CSCs phenotype (**Figure 3D-F**). Mammosphere cells were also CD24- (not shown). Vimentin staining was frequently observed indicating passage of a subpopulation through the epithelial to mesenchymal transition (EMT) (**Figure 3G**). These results suggest high enrichment in CTCs of the CSCs/EMT phenotype in mammospheres.

Drug treatment of mammospheres derived from CD45- cells

To demonstrate the fact that cultured CTCs reflect parental tumor sensitivity to therapeutic drugs, CD45- cells from TNBC patient 22 in mammosphere culture were treated with either

Table 1. Receptor status, diagnosis, stage, grade of primary tumor, metastasis sites and number of CD45-CK8+ or CD45-CK8- cells (per 10 million processed events) for selected breast cancer patients and a representative control volunteer (post-apheresis, post-FACS samples)

Patient number	ER	PR	HER2	Diagnosis	Grade	Stage	Metastasis	CD45-CK8- corrected for the number of processed events	CD45-CK8+ corrected for the number of processed events	Patient number
BC0003	+	+	-	IDC	2	IV	Bone	147434	180	3
BC0004	+	+	-	ILC	2	IV	Bone	24853	50	4
BC0005	+	+	-	IDC	2	IV	Bone, liver	903113	190	5
BC0011	+	+	-	ILC	2	IV	Bone	1877697	250	11
BC0028	+	+	-	IDC	2	III	na	210041	1620	28
BC0029	+	+	-	IDC	3	II	na	865812	750	29
BC0012	+	-	-	ILC	3	IV	Bone, lung, liver	130307	320	12
BC0013	+	-	-	ILC	2	IV	Bone, liver	234767	470	13
BC0008	+	+	+	IDC	2-3	IV	na	74365	250	8
BC0001	-	na	-	ILC	2	IV	Bone, lung	48244	3850	1
BC0009	-	-	-	IDC	3	III	Bone	1050512	260	9
BC0022	-	-	-	IP	2	I	-	241236	100	22
BC0027	-	-	-	IDC	3	I	-	130241	210	27
Control								74494	50	C

ILC: invasive lobular carcinoma. IDC: invasive ductal carcinoma. IP: invasive papilloma. na: not available.

taxol 10 nM, Herceptin 10 μg/ml or doxorubicin 10 uM for 48 hours. Cells were stained with an anti-CD45 Ab to check for absence of reactivity, then with 7-amino actinomycin D (7-AAD) viability dye, annexin V and analyzed by flow cytometry (**Figure 4**). Taxol and doxorubicin increased the proportion of apoptotic cells (lower right-hand gates) in treated mammospheres with respect to untreated controls. Consistent with the HER2-absent receptor status in a triple-negative patient, Herceptin had no apoptotic-inducing effect. These results show that cultured CTC-derived mammosheres react to therapeutic drugs in a manner consistent with that of primary tumors.

Xenografts

Mammospheres at third passage (6 weeks) were collected, trypsinised, and single cell suspensions from 5 patients (number 3, 5, 9, 12, 13, see **Table 1**) were injected in the mammary fat pads (MFP) or intratibially into 8-week old immunodeficient female SCID mice (10^4 cells/mouse, 5 mice/patient for MFP and 5 mice/patient for tibial injection). Contralateral MFPs or tibiae were sham injected. The animals were sacrificed 8 weeks after injection. Mammary tissue from animals with MFP injections was dissected and analyzed by H&E staining. Bones from animals with intratibial injections were stained with H&E staining and analysed by CT scan (**Figure 5**). 1 of 5 mice injected with cells from patients 9 (ER- PR- HER2-) and 13 (ER+ PR- HER2-) developed mammary pad tumors, 1 of 5 mice injected with cells from patient 12 (ER+ PR- HER2-) developed bone tumors, while mice injected with cells from patients 3 and 5 (ER+ PR+ HER2-) did not develop any tumors.

These results demonstrate that mammospheres derived from CTCs isolated through our platform can form tumors when injected in mammary fat pads or tibiae of athymic nude mice.

Next-generation sequencing of CTCs

Among BC patients who underwent apheresis and consented to participate, a 13-patient subpopulation was selected comprising one triple-positive patient, three triple-negative breast cancer (TNBC) patients, and the remainder being ER+ patients (**Table 1**). Cryopreserved post-apheresis post-Ficoll PBMC samples were stained with 4',6-diaminido-2-phenylindole (DAPI) and anti-CD45-APC-Cy antibody and separated by FACS. Re-selected gated living cells were stained with an anti-CK8-PercP-efluor 710 antibody and sorted by FACS-Aria into 4 subpopulations: CD45+CK8+, CD45+CK8-, CD45-CK8+, and CD45-CK8- (**Figure 6A-E**).

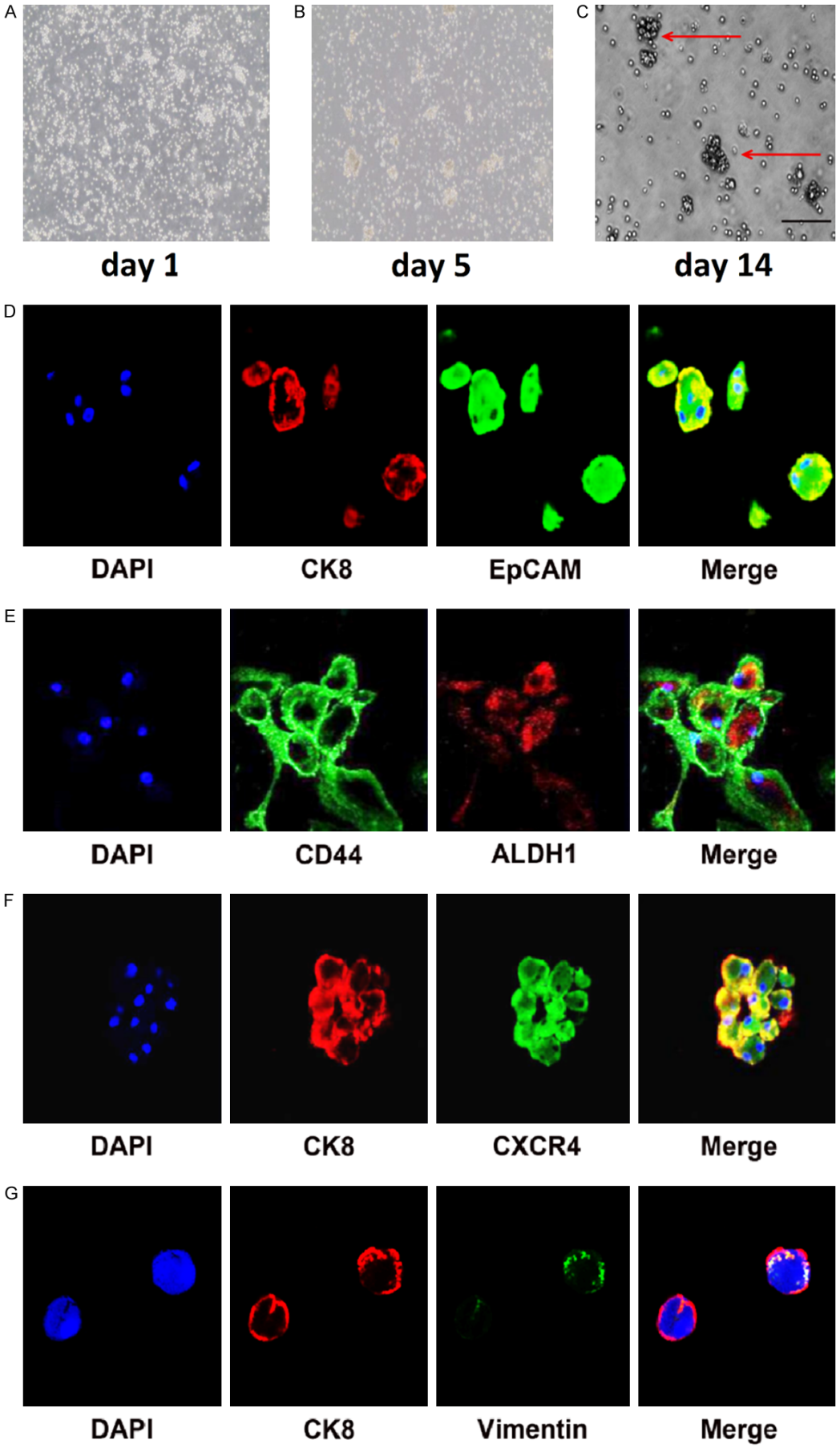
A
B
C
day 1
day 5
day 14
D
DAPI
CK8
EpCAM
Merge
E
DAPI
CD44
ALDH1
Merge
F
DAPI
CK8
CXCR4
Merge
G
DAPI
CK8
Vimentin
Merge

Figure 3. CD45- cells in mammosphere culture: isolated cells grown in mammocult medium in low-adherence plates at day 1 (A), day 5 (B), and day 14 (C). Red arrows indicate mammospheres. Immunofluorescent staining of mammospheres with (D) CK8, EpCAM, (E) CD44, ALDH1, (F) CK8, CXCR4 and (G) vimentin (from TNBC patient 22). Scale bar: 50 μm.

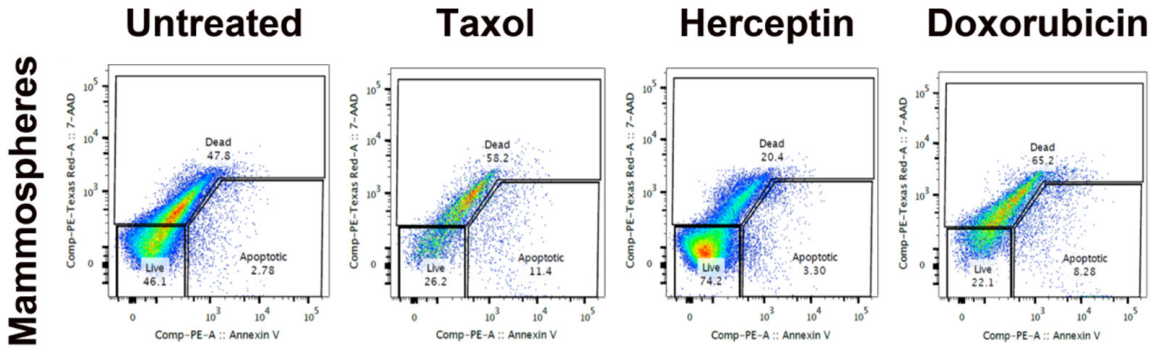

Figure 4. Flow analysis of cells from mammospheres treated in vitro for 48 h. With taxol (10 nM), Herceptin (10 μg/ml), or doxorubicin (10 μM). Cells were stained for annexin V and 7-AAD.

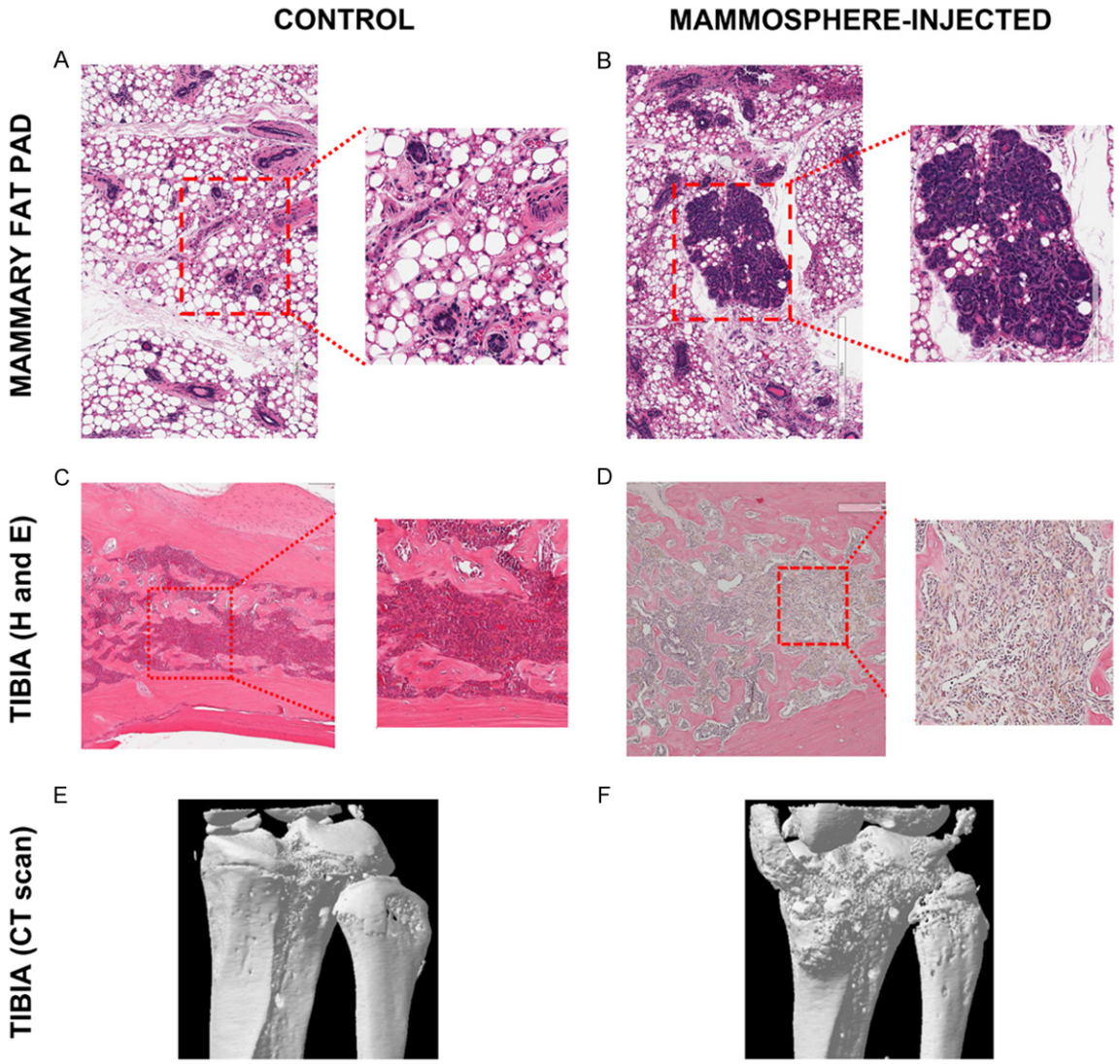

Figure 5. Xenografts of mammosphere-derived cells injected into nude mice sacrificed 8 weeks post-injection. Top row: H&E stain of mammary fat pad 8 weeks after sham injection (A) or injection of mammosphere cells (B). Middle row: H&E stain of tibia marrow 8 weeks after sham intratibial injection (C) or injection of mammosphere cells (D). Bottom row: CT scan of bone 8 weeks after sham injections (E) or injection of mammospheres (F). Mammophere cells were from patient 12 (ER+ PR- HER2-).

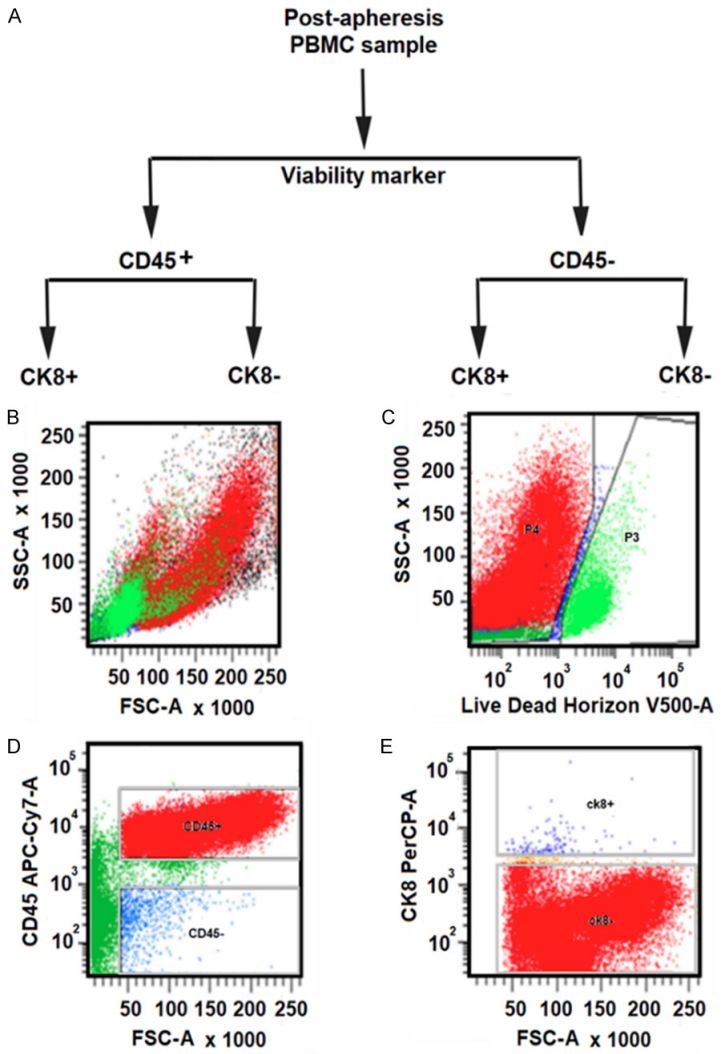

Figure 6. Representative FACS analysis of post-apheresis PMBC samples: (A) Diagram of separation strategy. (B-E) Subpopulations of PBMC sorted by FACS aria. (B) Forward and side scatter, (C) Staining with viability dye eFluor506 (P4 living cells, P3 dead cells), (D) FACS scan of living cells (P4) from (B) stained with eFluor506 and anti CD45-APC-Cy7 (top: CD45+ cells, bottom: CD45- cells), (E) FACS scan of CD45- cells from (D) stained with anti-CK8-PercP-efluor710 (top: CK8+, bottom: CK8-).

CD45-CK8+ and CD45-CK8- subpopulations counts were corrected for the number of processed events (**Table 1**). Blood from healthy volunteer women was also analysed as controls. The number of CK8+ cells in healthy volunteer controls was very low (at the limit of detection). The robustness of the method was tested by repeating measurements of CD45- fractions; the coefficient of variation was 3.8% for healthy volunteers controls and 8-15% for breast cancer patients.

Bulk RNA analysis

RNA was extracted from post-FACS subpopulations from all four subgroups (CD45+CK8+, CD45+CK8-, CD45-CK8+, and CD45-CK8-) obtained from breast cancer patient 22 (TNBC). cDNA was generated from aliquots and 200-cell and 1000-cell bulk analyses were conducted. The most variable 100 genes out of 500 are shown in **Figure 7**.

Large bulk analysis (1000 cells) regroups CD45+ cells away from CD45- groups (**Figure 7** lanes 1-5 and 8). N.B. Lanes 4-5 are replicates.

200 cell bulk analysis further refines the profile for CD45-CK8+ cells (CTCs) in the same patient into a visibly distinct group (**Figure 7** lanes 6 and 7, replicates). Lane 8 is a bioinformatically-generated pseudo-bulk sample that re-combines 35 single CD45-CK8+ cells, to illustrate how similar the single cell experiment is to the bulk analysis. Some genes appear as blanks in lane 8 because not enough cells are captures in the 35-cell sample to fill all gene expression that exists in 200-cell samples.

This approach illustrates high reproducibility between analyses of the same sample. The method is amenable to comparative analysis of the heterogeneous CTCs population for example, prior to and following chemotherapy. However, it makes a point for more precise expression analyses that can be achieved through single cell RNA analyses.

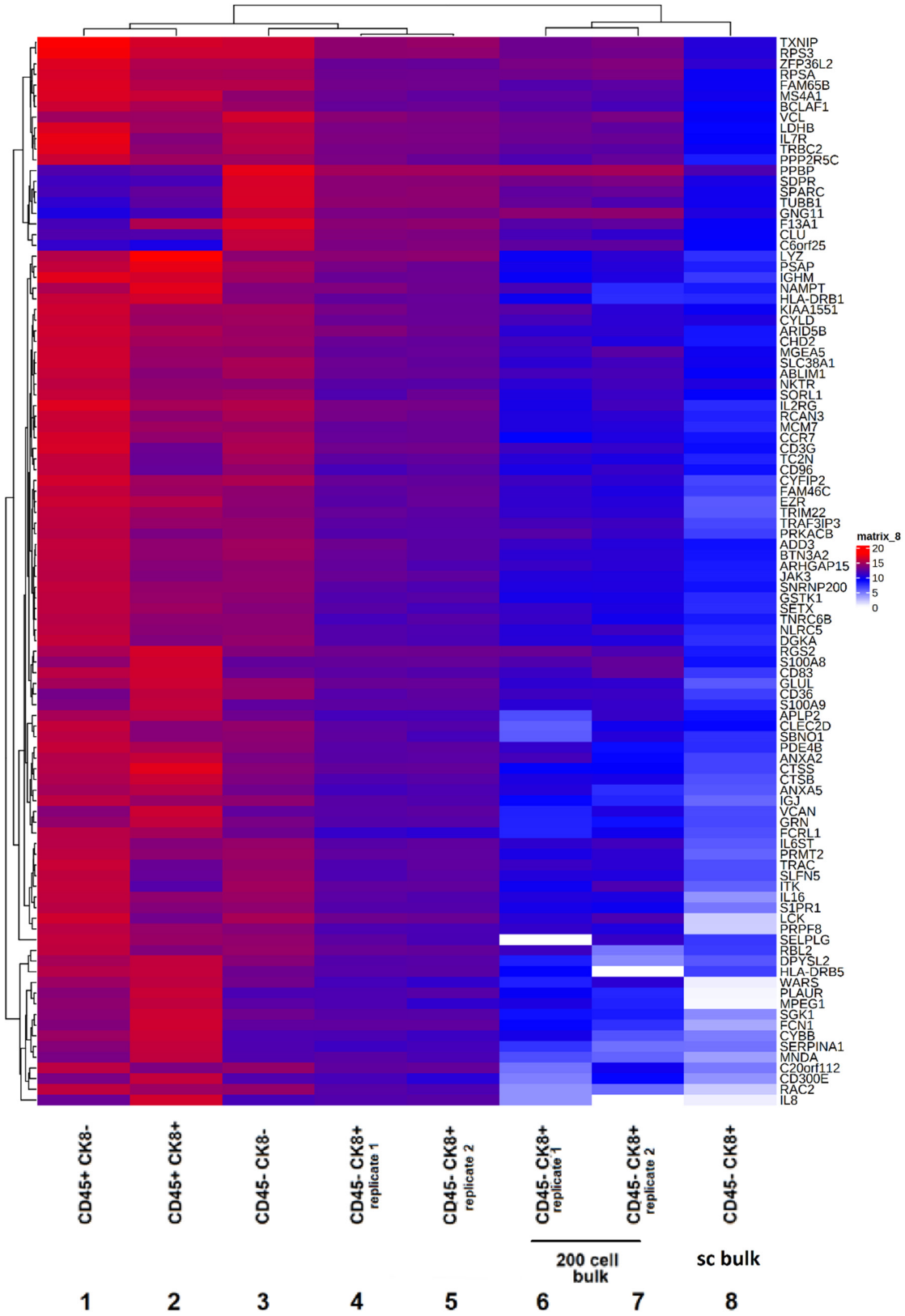

Figure 7. Bulk RNA sequencing of CTCs: bulk RNA sequencing analysis on all CTCs subpopulations from patient 22 (TNBC). Lanes 1-5 are 1000-cells bulk analyses. Lanes 6 and 7 are 200-cell bulk analysis. Lane 8 is a bioinformatically-generated sample of 35 combined single cell analyses. Column 4 and 5 are replicates of 1000 cells analyses, and 6 and 7 replicates of 200-cell analyses. The profile for the 100 most variable genes is illustrated.

A

	CD45+CK8-	CD45+CK8+	CD45-CK8-	CD45-CK8+
Diameter	7.439	8.881	5.796	7.721
Volume	0.216	0.367	0.102	0.241
Cells/μl	5,505	66	3,540	62

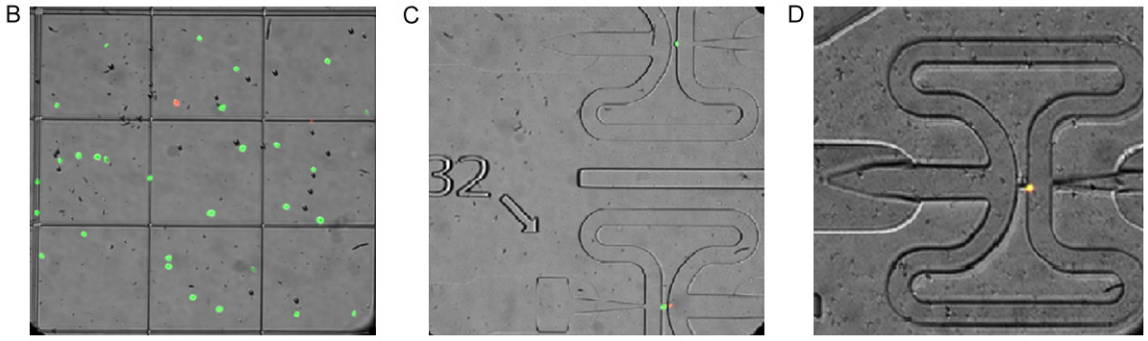

Figure 8. Size estimation and Fluidigm sorting: (A) Size of cells post-apheresis estimated by MoxiZ and numbers by FACS. (B) Viability staining (green) and CK staining (red). (C) Isolation on a Fluidigm chip of live cells (green) or cells positive for CK (red). (D) A cell that is both viable and positive for CK stains yellow.

Single-cell RNA analysis

To further qualify the CTC subpopulations displaying the highest potential for metastasis, single-cell RNA analysis was conducted on cells from patient 22 (TNBC) CD45-CK8+ population. Because all FACS Aria-sorted subpopulations displayed cell size between 5.7-8.9 micrometers (as estimated by Moxi Z chip **Figure 8A**), cells from any group could be successfully sorted and captured with a Fluidigm C1 instrument (Fluidigm, San Francisco, CA) equipped with the 5-10 micrometer Fluidigm C1 chip. Because of chip translucency, differently-stained cells can be identified and selected for subsequent analysis. Briefly, a 5 μl suspension of 200-1000 LiveStained CD45-CK8+ cells was loaded on the chip. Over 90% of CTCs were observed to remain viable (green), CK+ cells stained red, and viable cells positive for CK stained yellow (**Figure 8B-D**). Each sample yielded between 60 and 96 viable CK+ cells. Following capture, the cells were analysed within 4-6 minutes using an automated scanning fluorescent imaging system (EVOS FL, ThermoFisher), and single cells scored for viability and cytokeratin expression. Only live cells were used for RNA sequencing. Live cells were lysed in the chip, and cDNA synthesis initiated using the SMARTer amplification method (Clontech).

The cDNA from these CD45-CK8+ cells was used to prepare libraries for next generation sequencing by applying Nextera's tagmentation method, which is suitable for nanogram amounts of DNA. The libraries were sequenced using Illumina's HiSeq 2500 instrument at a rapid sequencing pipeline. We obtained a minimum of 1 million reads/single cell sample and >10 million from the 200 cell controls. From 3,000 to 12,000 transcripts could be detected from a single breast cancer-derived cell using a sequencing depth of 1-5 mi reads (**Figure 9A**). Saturation analysis indicates that reads per kilobase per million reads (RPKM) or fragments per kilobase per million reads (FPKM) values obtained at 2-4 mi reads are stable and allow relative quantification. Since one HiSeq 2500 flow cell can routinely yield over 200 mi reads, it is feasible to sequence 60-70 single cells/flow cell and obtain the required number of reads.

A comparison of the number of genes detected in 200-cell bulk and single cell (all CD45-CK8+) analysis indicates that it is possible by the present technique to detect a very high number of transcripts, comparable to results obtained from purified RNA (**Figure 9B**). A comparison was conducted in a 37-gene panel (with most variability) for bulk RNA results (200 CD45-

A

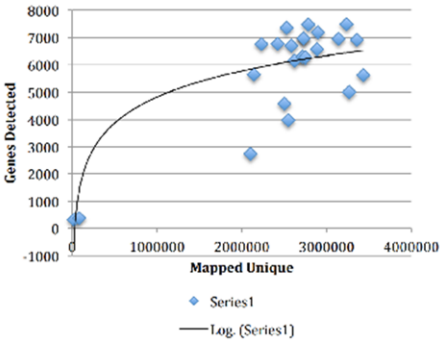

B

Samples analyzed by RNA- seq		
Type	Fraction	genes detected
single cell cDNA 35 cells	CD45 - CK8+	27770
200 cell cDNA	CD45 - CK8+ 1	14528
200 cell cDNA	CD45 - CK8+ 2	14863
RNA	CD45 - CK8+ 1	18573
RNA	CD45 - CK8+ 2	18355
RNA	CD45+ CK8 -	20273
RNA	CD45+ CK8+	21166
RNA	CD45+	17623
RNA	Cells before FACs	19201

C

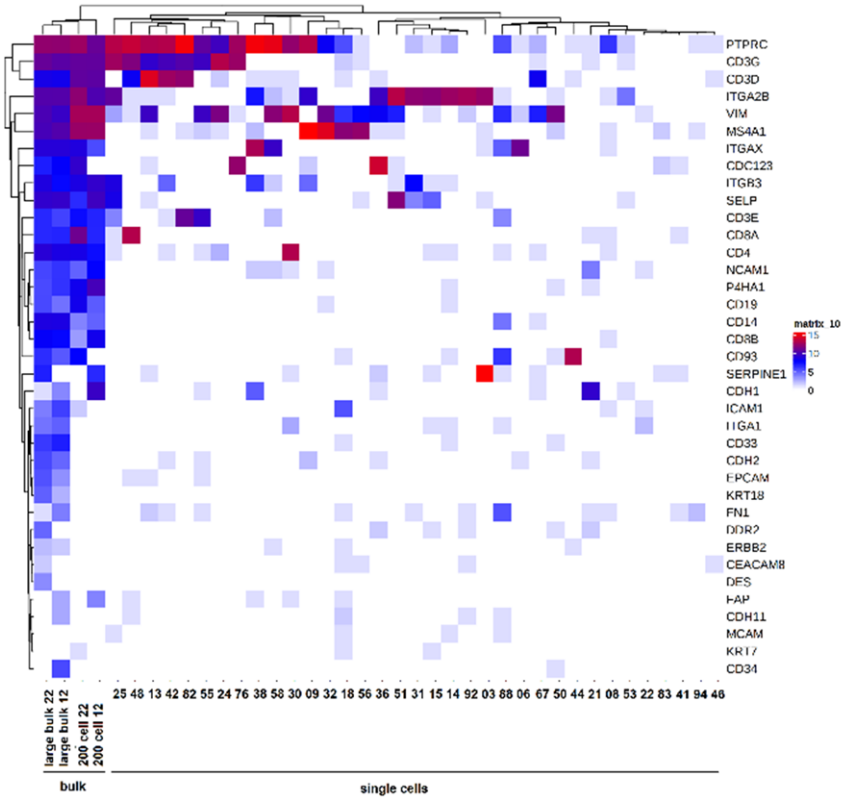

Figure 9. Bulk and single-cell RNA sequencing of CTCs: (A) Expected number of genes to be detected by single cell RNA sequencing. Black curve: log. (B) Number of genes detected by 200-cell bulk or single cell RNA sequencing of various fractions. (C) Clustering analysis obtained for large bulk (1000 cells), 200-cell bulk, and 35 individual CD45-CK8+ single cells from TNBC patient.

CK8+ cells) and for clustering of 35 single CD45-CK8+ cells (**Figure 9C**). Results indicate the presence of 5 or more separate clusters pointing to different profiles of cell sub-populations.

Analysis of markers for single cells compiled from current literature about CTCs indicates that cells fall into categories of epithelial, immune and mixed type (**Figure 10**).

In order to confirm distinct patterns in single cell analysis that are not discernable in bulk analyses, we examined the marker genes vimentin and platelet endothelial cell adhesion molecule (PECAM1 or CD31), as well as β-actin in single cells. Results for bulk analyses show expression of both vimentin and PECAM, however single cells are seen to express one or the other and rarely both, indicating heterogeneity of populations in CTCs (**Figure 11**).

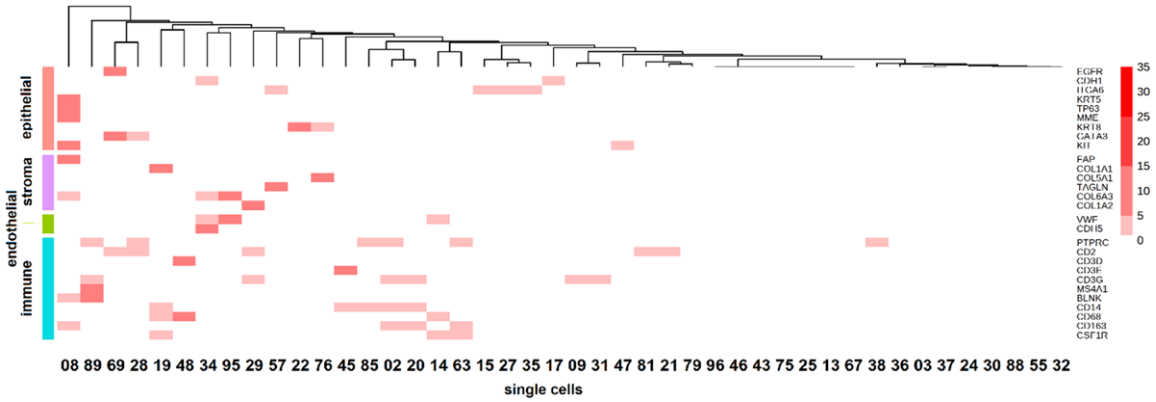

Figure 10. Analysis of markers for TNBC single cells indicates epithelial, immune and mixed signature.

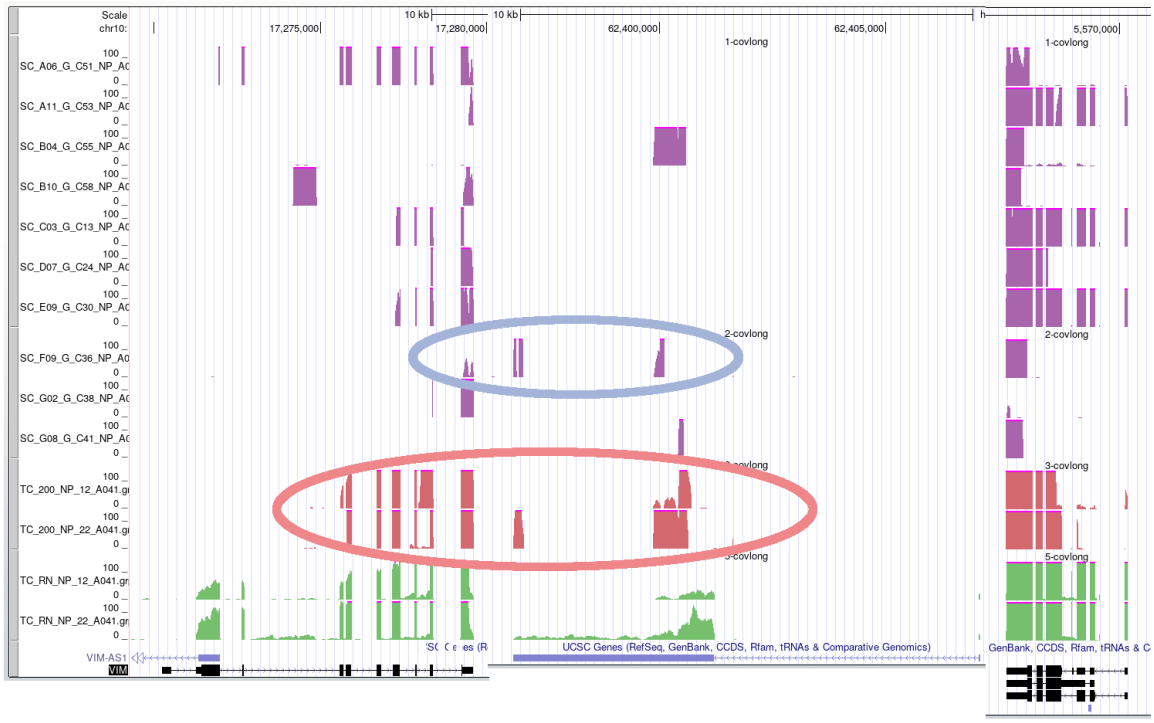

Figure 11. Detection of vimentin, PECAM1 and β-actin (ACTB) in single cells (purple) and bulk analyses (in red, direct cDNA synthesis; in green, cDNA synthesis after RNA extraction as a technical comparison) in the same CD45-CK8+ subpopulation. Genomic organization (introns and exons) for the 3 genes is projected from the UCSC genome browser (bottom). Vimentin and PECAM1 are both expressed in the bulk population (red oval) but are seldom expressed in the same individual cells (blue oval).

These results highlight the advantage of single cell sequencing over bulk analysis in identifying differential expression profiles within a single CTC population.

Discussion

The greatest challenge in CTC analysis is the very low abundance of these cells in peripheral blood. In order to counter CTC rarity and allow better analysis, we developed a large-scale, highly-reproducible apheresis-based purification platform to collect CTCs from peripheral blood. CTC detection from peripheral blood has been reported in a number of cancer types, such as lung [31], prostate [32], colorectal [33], breast [34], gastric [35] and biliary [36], however, some cancers such as pancreatic present inefficient CTC collection from peripheral sources due to hepatic filtration, and portal

vein samples have been used to provide better numbers [42]. Because of its enriching process, our proposed platform will likely be applicable to CTC collection of these rare samples through a cubital source.

The apheresis procedure described here affords a much higher CTC yield than is obtained from the usual 7.5 ml blood sample. The cells can be quantified, sorted and are suitable for subsequent *in vitro* and *in vivo* experimentation as well as for single-cell RNA analysis. Our protocol is based on CD45 negativity/CK8 positivity and therefore avoids eliminating many CTCs with metastatic ability. A frequent problem of EpCam-based purification methods. Through the early steps of our platform, we obtain a CD45 depleted fraction containing a population of cells that are enriched in CD45-CK8/18+ with a subfraction are ALDH1+, indicating substantial enrichment in cells displaying cancer stem cells characteristics.

CTCs are known to form clusters of two or more cells; this association results mostly from the aggregation of individual tumor cells [43] although cohesive shedding and collective migration also occurs [44]. Clusters display increased survival in the bloodstream and are up to 100 times more metastatic than single CTCs in breast cancer regardless of subtype or prior treatment [44]. Because the numbers of clusters is related to poor prognosis, their analysis can be used to monitor therapeutic progression. Importantly, clusters of cells bearing the cancer stem cell CD45- CK8/18+ and ALDH1+ phenotype are easily detected by our method.

Culturing mammary epithelial stem cells derived from primary breast tumors using non-adherent non-differentiating conditions produces cell aggregates (mammospheres) that enrich stem cells [45, 46]. Here, the CD45- cells isolated by our method were observed to grow as mammospheres in serum-free medium and display markers for CSCs (CK8, EpCam, ALDH1, CD44, and CXCR4) and for EMT (vimentin). For functional validation, mammospheres derived from patient CTCs were exposed to various therapeutic drugs. The cells reacted with apoptosis in a manner similar to that expected from the original primary tumor. For ex. mammospheres from a triple-negative patient reacted to Taxol and Doxorubicin but showed no response to Herceptin. We further observed that cells trypsinised from mammospheres can be successfully xenografted to produce tumors following mammary fat pad or intratibial injection into athymic nude mice. The system can be used for investigating the sensitivity of tumorigenic cells to various drugs as well as for further analysis of the tumor cell genotype.

When flow cytometry separation of post-apheresis PBMCs into 4 separate groups based on CD45 and CK8 status was followed by RNA analysis, we observed that robust RNA bulk sequencing results can be derived from small numbers of cells from the CD45-CK8+ subpopulation. Gene clustering analysis indicates that the CD45-CK8+ subpopulation displays an expression profile very distinct from the CD45+CK8+ and CD45+CK8- CTCs.

Cellular heterogeneity exists in the primary tumor with evidence of “patches” of tumor cells displaying different phenotypes. These cells shed into the circulation, resulting in a heterogeneous population of CTCs with varied invasive potential [47]. Limitations of current analysis approaches are linked to this high inherent heterogeneity of CTCs. Consequently, it is important to identify the CTC subpopulations displaying the highest potential for metastasis. RNA sequencing at the single cell level offers the possibility to identify distinct expression patterns that correlate with EMT and metastasis markers, as well as to highlight transcripts that can be assigned to distinct pathways potentially characteristic for individual subpopulations. Comparison of profiles for 35 single CD45-CK8+ cells to bulk RNA results for 200 CD45-CK8+ cells conducted in a 37-gene panel revealed the presence of 2 or 3 separate phenotype clusters, pointing to the feasibility of profile dissection of cell subpopulations.

Analysis of markers for TNBC single cells indicates epithelial, immune and mixed signatures. Furthermore, the marker genes vimentin and platelet endothelial cell adhesion molecule, (PECAM1 or CD31) as well as β-actin were examined in different single cells. Results for bulk analyses show expression of both vimentin and PECAM, however single cells are seen to express one or the other and rarely both, indicating heterogeneity of populations in CTCs

and highlighting the precision advantage of single cell over bulk analysis.

Future clinical applications for apheresis enrichment approaches that isolate CTCs in numbers significant enough will allow study of tumor evolution and intra-patient heterogeneity. Because the method is minimally-invasive and well-tolerated, serial procedures to follow disease evolution are also possible. An important clinical application of detailed CTC profiling is the identification of cells with high metastatic potential in real time, thereby providing a snapshot of tumor biology to guide drug selection at various cancer stages for optimised treatment. Another application is the screening of pharmaceutical compounds, which provides a unique opportunity to design personalized therapeutic interventions based on CTC molecular profile. The molecular characterization of CTCs may also lead to the discovery and identification of new targets for therapeutic intervention. Such approaches could include the targeting of specific overexpressed gene products and activated pathways that confer resistance to treatment, the identification of new targets, and the modulation of treatment as disease progresses.

Acknowledgements

This work is supported by grants from the United States Department of Defense (W81-XWH-15-1-0723) to RK, the Canadian Institutes of Health Research (MOP-142287) to RK, the Quebec Consortium for Drug Discovery to RK and CM and by Genome Canada (Genomic Paltform Grant) and CFI-LOF 32557 to JR. We thank Yu Chang Wang, Génome Québec Innovation Centre, for technical assistance, Josée Girouard, R.N., Centre for Innovative Medicine, MUHC, for conducting apheresis procedures, Anna Lisa Tedeschi, Professional Affiliate, MUHC Research Institute, for administrative help and Ramy Saleh for assistance as a research coordinator of the study. We also thank Francesca Kanapathy-Sinnaiaha, Jing Lian, Benoit Ochietti, Nicholas Rozza and Karine Sellin of the MUHC Research Institute for their excellent technical assistance in the development of the platform.

Disclosure of conflict of interest

None.

Abbreviations

ALDH1, aldehyde dehydrogenase 1; 7-AAD, 7-amino-actinomycin D; CD, cluster of differentiation; CK, cytokeratin; CTC, circulating tumor cell; DAPI, 4',6-diamidino-2-phenylindole; EMT, epithelial-to-mesenchymal transition; EpCAM, epithelial cell adhesion molecule; FACS, fluorescence-activated cell sorting; IHC, immunohistochemistry; H&E, hematoxylin and eosin; MFP, mammary fay pad; PBMC, peripheral blood mononuclear cell; PECAM1, platelet endothelial cell adhesion molecule precursor; RNA seq, RNA sequencing; SCID, severe combined immunodeficient mice; WBC, white blood cell.

Address correspondence to: Richard Kremer and Catalin Mihalcioiu, Department of Medicine, McGill University Health Centre, Glen Site, 1001 Boul. Décarie, Mail Drop EM1.3229, Montréal, Québec, H4A 3J1, Canada. E-mail: richard.kremer@mcgill.ca (RK); catalin.mihalcioiu@muhc.mcgill.ca (CM)

References

[1] Plaks V, Koopman CD and Werb Z. Circulating tumor cells. Science 2013; 341: 1186-1188.
[2] Micalizzi DS, Maheswaran S and Haber DA. A conduit to metastasis: circulating tumor cell biology. Genes Dev 2017; 31: 1827-1840.
[3] Williams SC. Circulating tumor cells. Proc Natl Acad Sci U S A 2013; 110: 4861-4861.
[4] Toss A, Mu Z, Fernandez S and Cristofanilli M. CTC enumeration and characterization: moving toward personalized medicine. Ann Transl Med 2014; 2: 108.
[5] Wallwiener M, Riethdorf S, Hartkopf AD, Modugno C, Nees J, Madhavan D, Sprick MR, Schott S, Domschke C and Baccelli I. Serial enumeration of circulating tumor cells predicts treatment response and prognosis in metastatic breast cancer: a prospective study in 393 patients. BMC Cancer 2014; 14: 1.
[6] Hall C, Karhade M, Laubacher B, Anderson A, Kuerer H, DeSynder S and Lucci A. Circulating tumor cells after neoadjuvant chemotherapy in stage I-III triple-negative breast cancer. Ann Surg Oncol 2015; 22: 552-558.
[7] Lucci A, Hall CS, Lodhi AK, Bhattacharyya A, Anderson AE, Xiao L, Bedrosian I, Kuerer HM and Krishnamurthy S. Circulating tumour cells in non-metastatic breast cancer: a prospective study. Lancet Oncol 2012; 13: 688-695.
[8] Pierga JY, Bidard FC, Autret A, Petit T, Andre F, Dalenc F, Levy C, Ferrero JM, Romieu G and Bonneterre J. Circulating tumour cells and

pathological complete response: independent prognostic factors in inflammatory breast cancer in a pooled analysis of two multicentre phase II trials (BEVERLY-1 and -2) of neoadjuvant chemotherapy combined with bevacizumab. Ann Oncol 2017; 28: 103-109.
[9] Cohen SJ, Punt CJ, Iannotti N, Saidman BH, Sabbath KD, Gabrail NY, Picus J, Morse M, Mitchell E and Miller MC. Relationship of circulating tumor cells to tumor response, progression-free survival, and overall survival in patients with metastatic colorectal cancer. J Clin Oncol 2008; 26: 3213-3221.
[10] de Bono JS, Scher HI, Montgomery RB, Parker C, Miller MC, Tissing H, Doyle GV, Terstappen LW, Pienta KJ and Raghavan D. Circulating tumor cells predict survival benefit from treatment in metastatic castration-resistant prostate cancer. Clin Cancer Res 2008; 14: 6302-6309.
[11] Liu MC, Shields PG, Warren RD, Cohen P, Wilkinson M, Ottaviano YL, Rao SB, Eng-Wong J, Seillier-Moiseiwitsch F and Noone AM. Circulating tumor cells: a useful predictor of treatment efficacy in metastatic breast cancer. J Clin Oncol 2009; 27: 5153-5159.
[12] Koch C, Kuske A, Joosse SA, Yigit G, Sflomos G, Thaler S, Smit DJ, Werner S, Borgmann K and Gärtner S. Characterization of circulating breast cancer cells with tumorigenic and metastatic capacity. EMBO Mol Med 2020; 12: e11908.
[13] Klinac D, Gray ES, Freeman JB, Reid A, Bowyer S, Millward M and Ziman M. Monitoring changes in circulating tumour cells as a prognostic indicator of overall survival and treatment response in patients with metastatic melanoma. BMC Cancer 2014; 14: 1.
[14] Miyamoto DT, Sequist LV and Lee RJ. Circulating tumour cells [mdash] monitoring treatment response in prostate cancer. Nat Rev Clin Oncol 2014; 11: 401-412.
[15] Baccelli I, Schneeweiss A, Riethdorf S, Stenzinger A, Schillert A, Vogel V, Klein C, Saini M, Bäuerle T and Wallwiener M. Identification of a population of blood circulating tumor cells from breast cancer patients that initiates metastasis in a xenograft assay. Nat Biotechnol 2013; 31: 539-544.
[16] Barriere G, Fici P, Gallerani G, Fabbri F, Zoli W and Rigaud M. Circulating tumor cells and epithelial, mesenchymal and stemness markers: characterization of cell subpopulations. Ann Transl Med 2014; 2: 109.
[17] Yang MH, Imrali A and Heeschen C. Circulating cancer stem cells: the importance to select. Chin J Cancer Res 2015; 27: 437.
[18] Agnoletto C, Corrà F, Minotti L, Baldassari F, Crudele F, Cook WJJ, Di Leva G, d'Adamo AP, Gasparini P and Volinia S. Heterogeneity in circulating tumor cells: the relevance of the stem-cell subset. Cancers 2019; 11: 483.
[19] Shibue T and Weinberg RA. EMT, CSCs, and drug resistance: the mechanistic link and clinical implications. Nat Rev Clin Oncol 2017; 14: 611.
[20] Jie XX, Zhang XY and Xu CJ. Epithelial-to-mesenchymal transition, circulating tumor cells and cancer metastasis: mechanisms and clinical applications. Oncotarget 2017; 8: 81558.
[21] Yan WT, Cui X, Chen Q, Li YF, Cui YH, Wang Y and Jiang J. Circulating tumor cell status monitors the treatment responses in breast cancer patients: a meta-analysis. Sci Rep 2017; 7: 1-12.
[22] Man Y, Wang Q and Kemmner W. Currently used markers for CTC isolation-advantages, limitations and impact on cancer prognosis. J Clin Exp Pathol 2012; 2011: 102.
[23] Soysal SD, Muenst S, Barbie T, Fleming T, Gao F, Spizzo G, Oertli D, Viehl CT, Obermann EC and Gillanders WE. EpCAM expression varies significantly and is differentially associated with prognosis in the luminal B HER2+, basal-like, and HER2 intrinsic subtypes of breast cancer. Br J Cancer 2013; 108: 1480-1487.
[24] Hyun KA, Koo GB, Han H, Sohn J, Choi W, Kim SI, Jung HI and Kim YS. Epithelial-to-mesenchymal transition leads to loss of EpCAM and different physical properties in circulating tumor cells from metastatic breast cancer. Oncotarget 2016; 7: 24677.
[25] Kagan M, Howard D, Bendele T, Mayes J, Silvia J, Repollet M, Doyle J, Allard J, Tu N and Bui T. A sample preparation and analysis system for identification of circulating tumor cells. J Clin Ligand Assay 2002; 25: 104-110.
[26] Joosse SA, Hannemann J, Spötter J, Bauche A, Andreas A, Müller V and Pantel K. Changes in keratin expression during metastatic progression of breast cancer: impact on the detection of circulating tumor cells. Clin Cancer Res 2012; 18: 993-1003.
[27] Schwartz J, Winters JL, Padmanabhan A, Balogun RA, Delaney M, Linenberger ML, Szczepiorkowski ZM, Williams ME, Wu Y and Shaz BH. Guidelines on the use of therapeutic apheresis in clinical practice-evidence-based approach from the writing committee of the American Society for Apheresis: the Sixth Special Issue. J Clin Apheresis 2013; 28: 145-284.
[28] Li H, Meng QH, Noh H, Batth IS, Somaiah N, Torres KE, Xia X, Wang R and Li S. Detection of circulating tumor cells from cryopreserved human sarcoma peripheral blood mononuclear cells. Cancer Lett 2017; 403: 216-223.
[29] Greene B, Hughes A and King M. Circulating tumor cells: the substrate of personalized medicine? Front Oncol 2012; 2: 69.

[30] Solano C, Badia B, Lluch A, Marugan I, Benet I, Arbona C, Prosper F and Garcia-Conde J. Prognostic significance of the immunocytochemical detection of contaminating tumor cells (CTC) in apheresis products of patients with high-risk breast cancer treated with high-dose chemotherapy and stem cell transplantation. Bone Marrow Transplant 2001; 27: 287-93.
[31] Zhang Z, Shiratsuchi H, Lin J, Chen G, Reddy RM, Azizi E, Fouladdel S, Chang AC, Lin L and Jiang H. Expansion of CTCs from early stage lung cancer patients using a microfluidic co-culture model. Oncotarget 2014; 5: 12383.
[32] Hu B, Rochefort H and Goldkorn A. Circulating tumor cells in prostate cancer. Cancers 2013; 5: 1676-1690.
[33] Kuboki Y, Matsusaka S, Minowa S, Shibata H, Suenaga M, Shinozaki E, Mizunuma N, Ueno M, Yamaguchi T and Hatake K. Circulating tumor cell (CTC) count and epithelial growth factor receptor expression on CTCs as biomarkers for cetuximab efficacy in advanced colorectal cancer. Anticancer Res 2013; 33: 3905-3910.
[34] Riethdorf S, Fritsche H, Müller V, Rau T, Schindlbeck C, Rack B, Janni W, Coith C, Beck K and Jänicke F. Detection of circulating tumor cells in peripheral blood of patients with metastatic breast cancer: a validation study of the CellSearch system. Clin Cancer Res 2007; 13: 920-928.
[35] Tsujiura M, Ichikawa D, Konishi H, Komatsu S, Shiozaki A and Otsuji E. Liquid biopsy of gastric cancer patients: circulating tumor cells and cell-free nucleic acids. World J Gastroenterol 2014; 20: 3265.
[36] Al Ustwani O, Iancu D, Yacoub R and Iyer R. Detection of circulating tumor cells in cancers of biliary origin. J Gastrointest Oncol 2012; 3: 97.
[37] Fehm TN, Meier-Stiegen F, Driemel C, Jäger B, Reinhardt F, Naskou J, Franken A, Neubauer H, Neves RP and van Dalum G. Diagnostic leukapheresis for CTC analysis in breast cancer patients: CTC frequency, clinical experiences and recommendations for standardized reporting. Cytometry Part A 2018; 93: 1213-1219.
[38] Fischer JC, Niederacher D, Topp SA, Honisch E, Schumacher S, Schmitz N, Föhrding LZ, Vay C, Hoffmann I and Kasprowicz NS. Diagnostic leukapheresis enables reliable detection of circulating tumor cells of nonmetastatic cancer patients. Proc Natl Acad Sci U S A 2013; 110: 16580-16585.
[39] Philip J, Sarkar RS and Pathak A. Adverse events associated with apheresis procedures: incidence and relative frequency. Asian J Transfus Sci 2013; 7: 37.
[40] Weaver BA. How Taxol/paclitaxel kills cancer cells. Mol Biol Cell 2014; 25: 2677-2681.
[41] Li J, Camirand A, Zakikhani M, Sellin K, Guo Y, Luan X, Mihalcioiu C and Kremer R. Parathyroid hormone-related protein inhibition blocks triple-negative breast cancer expansion in bone through epithelial to mesenchymal transition reversal. JBMR Plus 2022; 6: e10587.
[42] Catenacci DV, Chapman CG, Xu P, Koons A, Konda VJ, Siddiqui UD and Waxman I. Acquisition of portal venous circulating tumor cells from patients with pancreaticobiliary cancers by endoscopic ultrasound. Gastroenterology 2015; 149: 1794-1803, e1794.
[43] Liu X, Taftaf R, Kawaguchi M, Chang YF, Chen W, Entenberg D, Zhang Y, Gerratana L, Huang S and Patel DB. Homophilic CD44 interactions mediate tumor cell aggregation and polyclonal metastasis in patient-derived breast cancer models. Cancer Discov 2019; 9: 96-113.
[44] Schuster E, Taftaf R, Reduzzi C, Albert MK, Romero-Calvo I and Liu H. Better together: circulating tumor cell clustering in metastatic cancer. Trends Cancer 2021; 7: 1020-1032.
[45] Wang R, Lv Q, Meng W, Tan Q, Zhang S, Mo X and Yang X. Comparison of mammosphere formation from breast cancer cell lines and primary breast tumors. J Thorac Dis 2014; 6: 829.
[46] Dontu G, Abdallah WM, Foley JM, Jackson KW, Clarke MF, Kawamura MJ and Wicha MS. In vitro propagation and transcriptional profiling of human mammary stem/progenitor cells. Genes Dev 2003; 17: 1253-1270.
[47] Vismara M, Reduzzi C, Daidone MG and Cappelletti V. Circulating Tumor Cells (CTCs) heterogeneity in metastatic breast cancer: different approaches for different needs. Adv Exp Med Biol 2020; 1220: 81.